

On the influence of resonant absorption on the iron emission line profiles from accreting black holes

Mateusz Ruszkowski and Andrew C. Fabian

Institute of Astronomy, Madingley Road, Cambridge CB3 0HA

23 September 2018

ABSTRACT

The fluorescent iron $K\alpha$ emission line profile provides an excellent probe of the innermost regions of active galactic nuclei. Fe XXV and Fe XXVI in diffuse plasma above the accretion disc can affect the X-ray spectrum by iron $K\alpha$ resonant absorption. This in turn can influence the interpretation of the data and the estimation of the accretion disc and black hole parameters. We embark on a fully relativistic computation of this effect and calculate the iron line profile in the framework of a specific model in which rotating, highly ionized and resonantly-absorbing plasma occurs close to the black hole. This can explain the features seen in the iron $K\alpha$ line profile recently obtained by Nandra et al. (1999) for the Seyfert 1 galaxy NGC 3516. We show that the redshift of this feature can be mainly gravitational in origin and accounted for without the need to invoke fast accretion of matter onto the black hole. New X-ray satellites such as XMM, ASTRO-E and Chandra provide excellent opportunities to test the model against high quality observational data.

Key words: accretion, accretion discs - black hole physics - galaxies: active - galaxies: Seyfert - X-rays: galaxies, line: formation - galaxies

1 INTRODUCTION

The fluorescent $K\alpha$ iron emission line has been observed in many active galactic nuclei and shown to possess a broad and redshifted profile (Fabian et. al 1994, Mushotzky et al. 1995, Tanaka et al. 1995, Reynolds 1997, Nandra et. al 1997). It has been demonstrated, for example, in the best studied case of the Seyfert 1 galaxy MCG-6-30-15, that the strong continuum variability is accompanied by changes in the iron line itself (Iwasawa et al. 1996, Lee et al. 1999). These results show that the fluorescent Fe $K\alpha$ line originates from the very central parts of the accretion disc close to the black hole, giving a natural explanation for both the rapid variability and the strong redshift detected in these objects. This opens a unique opportunity constrain the spin of the black hole, its mass and the structure of the accretion disc.

Recently Nandra et. al (1999) reported on a long ASCA observation of the Seyfert 1 galaxy NGC 3516. Their integrated iron line profile contains a factor of ~ 3.5 times more photons than that of MCG-6-30-15 and therefore at the present time provides an excellent opportunity to study the central parts of an active nucleus. Nandra et al. (1999) found tentative evidence for a redshifted absorption feature superimposed on the emission line profile. They interpret it as being consistent with resonant scattering in infalling material. Motivated by such an interesting possibility, we em-

bark on theoretical modelling of a similar effect. The crucial ingredient of our model is a strong gravitational field and therefore we fully account for all relevant general relativistic effects. We assume that the black hole and the central parts of the accretion disc are embedded in a cloud of hot, rapidly rotating and highly ionized plasma in which iron is not totally stripped of all electrons. Hydrogen and helium-like iron ions are then capable of producing significant absorption and thus of changing the shape of the disc emission line profile. If confirmed by further observations, this effect would suggest that future high quality data should be analyzed with the possibility of resonant absorption in mind, as the presence of optically-thin material surrounding the central region of an AGN could modify the emission line profile and therefore affect the interpretation of such data. The presence of the absorption features can also shed new light on the properties of the accretion flow near black holes, as the position of the gravitationally redshifted absorption line will additionally depend on the velocity pattern close to the black hole.

The paper is organized as follows: the next section contains the description of our approach to calculate the absorption features. Section 3 is devoted to the general presentation and discussion of our results and also contains a discussion of the iron line shape in the context of the recently obtained iron line profiles of NGC 3516 by Nandra et. al (1999).

2 DESCRIPTION OF THE METHOD AND BASIC ASSUMPTIONS

We assume that the accretion disc is optically thick and geometrically thin and that the primary source of X-ray radiation is a hot and optically thin corona located just above the accretion disc. The central black hole and the accretion disc with the corona are embedded in a cooler ($\sim 10^7 - 10^8$ K), extended cloud of plasma (see Fig. 1). The primary power law flux is incident on the disc and produces fluorescent photons. The fluorescent line and continuum photons then pass through and may interact with such plasma. Under such conditions a significant fraction of iron ions are in the hydrogen (Fe XXVI) and helium-like (Fe XXV) states. These ions can resonantly absorb the fluorescent line and continuum photons emerging from the accretion disc and corona. The permitted transitions of interest are $1s(^2S) - 2p(^2P)$ of H-like iron ($E_{\text{H}} = 6.9$ keV) and $1s^2(^1S) - 1s2p(^1P)$ of He-like iron ($E_{\text{He}} = 6.7$ keV) with the large oscillator strengths f_{lu} equal 0.416 for H-like and 0.794 for He-like (Kato 1976). This means that absorption lines can potentially change the shape of the observed broad iron line profile which is generated in the accretion disc with the rest energy $E_{\text{disc}} = 6.4$ keV.

2.1 The optical depth

We now proceed to describe the calculation method for the optical depth of resonant absorption. We first estimate the characteristic distance λ_{Sob} over which the energy of a photon, as seen by an observer who is at rest with the hot plasma, changes by the Doppler thermal width $\Delta\nu_{\text{D}} = (\nu_{\text{abs}}/c)(2kT/Am_{\text{p}})^{1/2}$, where m_{p} is a mass of a proton, A stands for the ion mass number and ν_{abs} is the frequency of the absorption line. We use the equation (Novikov & Thorne, 1973):

$$\left| \frac{dl}{d\nu} \right| = (|\nu_{\text{abs}}(p_{\mu}u^{\mu})_{;\alpha}p^{\alpha}|)^{-1} \equiv \lambda = \frac{\lambda_{\text{Sob}}}{\Delta\nu_{\text{D}}}, \quad (1)$$

where l is the proper length as measured in the local rest frame of the plasma flow. This frame-independent equation is derived easily by geometrical arguments in the locally non-rotating frame. In the above equation p_{μ} is the 4-momentum of a photon, u^{μ} is the 4-velocity of the absorbing medium and ν_{abs} is the rest frequency of the absorption line. We choose the velocity field u^{μ} to be of the form:

$$\mathbf{u} = C(\partial_t + \Omega\partial_{\phi}), \quad (2)$$

where

$$C = (-g_{tt} - 2\Omega g_{t\phi} - \Omega^2 g_{\phi\phi})^{-1/2} \quad (3)$$

and $\Omega = u^{\phi}/u^t$ is the angular velocity of the absorbing medium as seen at infinity. Note that the choice of Ω cannot be arbitrary and certainly the angular velocity must be constrained by the causality condition: $g_{tt} + 2\Omega g_{t\phi} + \Omega^2 g_{\phi\phi} < 0$. For example, note that the assumption of constant specific angular momentum $l_s \equiv -u_{\phi}/u_t$ on spheres of fixed r in Boyer-Lindquist coordinates (Kurpiewski & Jaroszyński 1999) violates this condition. Therefore, in our simulations we adopt the following definition of Ω :

$$\Omega = \left(\frac{\theta}{\pi/2} \right) \Omega_{\text{K}} + \left[1 - \left(\frac{\theta}{\pi/2} \right) \right] \omega, \quad (4)$$

where θ is the poloidal Boyer-Lindquist coordinate, $\Omega_{\text{K}} = (r^{3/2} + a)^{-1}$ is the Keplerian angular velocity and ω is the angular velocity of the gravitational drag, i.e. we assume that the hot plasma follows the velocity of the disc close to its surface and gradually changes its angular velocity to reach the value ω on the polar axis (note that at the black hole horizon radius $\Omega = \omega$ for all θ). From Eq. 1 we get:

$$\lambda_{\text{Sob}} = \frac{1}{c} \left(\frac{2kT}{Am_{\text{p}}} \right)^{1/2} \lambda = 5.7 \times 10^{-4} \left(\frac{T}{10^8 \text{K}} \right)^{1/2} \lambda, \quad (5)$$

It has been checked numerically that for the overwhelming majority of trajectories connecting the accretion disc and the observer (for different inclinations of the disc) $\lambda_{\text{Sob}} \ll \lambda_c$, where λ_c is a characteristic length scale over which the density remains roughly constant. However in our calculations we assume that the cloud has a uniform density distribution n_{H} in the local rest frame within a given radius R_c (i.e. $\lambda_c = R_c$). In the real situation, the absorption feature is likely to be variable (as indeed observed by Nandra et al. 1999) and the density distribution may correspond to an unstable configuration with a clumpy structure. Since we only intend to show what the temporal shape of the line might be, we argue that at the present stage it is not necessary to consider a more sophisticated density distribution corresponding to a stable configuration. The above constraints on λ_{Sob} ensure that we may use the Sobolev approximation to describe the resonant absorption in the plasma, i.e. we may assume that the absorption occurs locally and that the medium is transparent for most of the trajectory of a photon with a given emission energy. Thus in the further analysis we model the absorption line as a Dirac delta function. The optical depth per absorption event is then given by the formula (compare with Castor 1970, Shu 1991):

$$\tau = 5.5 \times 10^{-2} \left(\frac{E_{\text{abs}}}{6.7 \text{keV}} \right)^{-1} \left(\frac{A_{\text{Fe}}}{2A_{\text{Fe}\odot}} \right) \left(\frac{f_{\text{lu}}}{0.5} \right) \times \left(\frac{f_1 N_{\text{H}}}{10^{23} \text{cm}^{-2}} \right) \left(\frac{\lambda}{R_c} \right), \quad (6)$$

where E_{abs} is the rest energy of the absorption line, A_{Fe} is the abundance of iron (the solar abundance of iron is $A_{\text{Fe}\odot} = 3.3 \times 10^{-5}$, Morrison & McCammon 1983), f_1 is the fraction of ions in the H-like or He-like state, f_{lu} is the absorption oscillator strength and $N_{\text{H}} (\equiv n_{\text{H}} R_c)$ is the parameter related to the column density. We checked that although for some photon trajectories, energies and adopted values of N_{H} , the optical depth for resonant absorption may exceed unity, the depth of the observed continuum absorption feature varies almost linearly with N_{H} (for different inclinations of the disc) implying that we are effectively dealing with optically-thin resonant absorption.

2.2 The iron line profile

2.2.1 The absorption of the continuum and the emission line

The overall iron line profile was calculated in two steps. In the first step we calculated the shape of the partially absorbed fluorescent emission line generated in the disc and, superimposed on it, the resonant absorption feature due to the continuum absorbed by the hot cloud surrounding

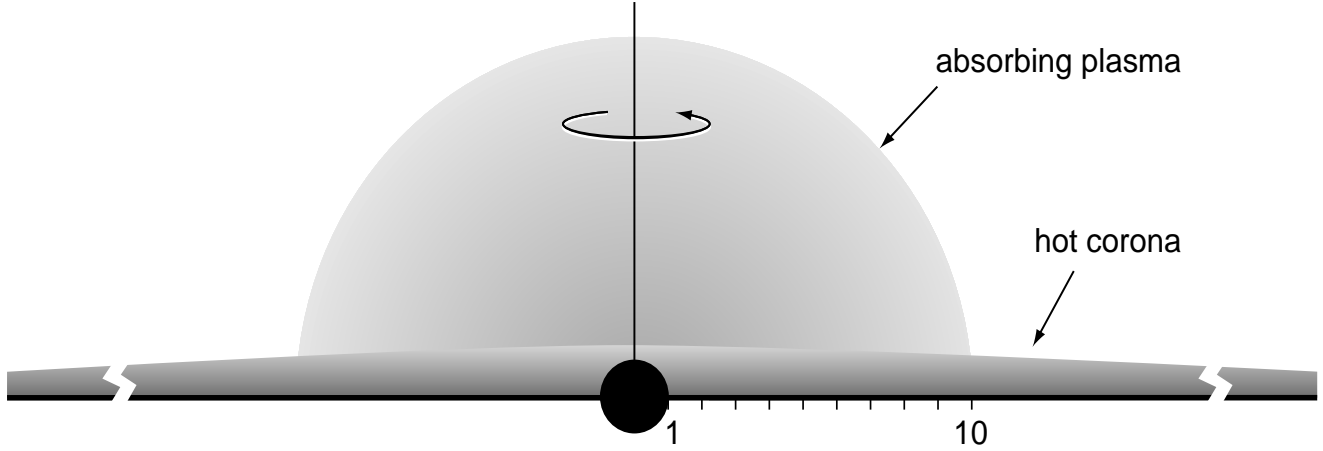


Figure 1. The assumed geometry of the central region

the disc. We assumed that the continuum was generated in the corona located just above the accretion disc. We used the ray back-tracing method and searched for the absorption regions corresponding to all energies of the continuum photons and the fluorescent line photons and calculated the optical depth as a function of energy for each photon trajectory. We then accumulated the optical depths when multiple absorption points occurred for the same energy. The line energy flux relative to the continuum for a given pixel element on the observer's image plane F_{line} was calculated from the following formula:

$$F_{\text{line}}(E_{\text{obs}})dE_{\text{obs}} = \left[g_{\text{t}}^4 \Delta I(E_{\text{obs}}/g_{\text{t}}) \exp\left(-\sum \tau\right) EW_{\text{em}} + -g_{\text{t}}^3 I_{\text{c}}(E_{\text{obs}}/g_{\text{t}}) \left(1 - \exp\left(-\sum \tau\right)\right) dE_{\text{obs}} \sec \beta \right] \frac{dxdy}{r_0^2}, \quad (7)$$

where $\Delta I(6.4\text{keV}) = I_{\text{c}}(6.4\text{keV})$ and 0 otherwise, EW_{em} is the equivalent width of the disc emission line from the disc element as seen face on in the local rest frame, g_{t} is the total redshift factor, β is the angle between the direction perpendicular to the disc and the direction of emitted photons as measured by the comoving observer and the last factor represents the solid angle subtended by the pixel on the observer's image plane. The continuum intensity I_{c} in the above equation is given by $I_{\text{c}} = \frac{1}{\pi}(\varepsilon(R)/2)$, where $\varepsilon(R) \propto R^{-\Gamma} E_{\text{em}}^{-\alpha}$ is the total X-ray emissivity of the corona at the distance R from the centre. The second component in the above equation describes absorption of the continuum photons, whereas the first corresponds to the absorption of the disc emission line measured relative to the continuum. The $\sec \beta$ factor accounts for the isotropy of radiation from the corona which was assumed to be optically thin.

2.2.2 Correction for spontaneous emission following absorption

Resonant absorption is a scattering process and therefore in our case is followed by de-excitation of the iron ions rather than destruction of photons. This effect will of course partially cancel the absorption features. The importance of this effect may be estimated for the case of a point-like source in the geometrical centre of the disc. Such estimation may be

reasonable if the emissivity index of the disc is steep. However at this stage we need this assumption only to estimate the order of magnitude of this effect. In such a situation the emission line flux F_{dex} is given by (see Matt 1994):

$$F_{\text{dex}} = 0.5 F_{\text{abs}} Y_{i-1} \left(\frac{\Delta\Omega/4\pi}{0.5} \right), \quad (8)$$

where F_{abs} is the absorbed flux and Y_{i-1} is the probability that the absorption is followed by a spontaneous emission rather than autoionization (where appropriate) and thus destruction of the photon. This probability can be approximated as the fluorescent yield of the previous ion (Band et al. 1990) and equals 1 in the case of H and He-like iron ions. Taking into account the assumed geometry of the system, $\Delta\Omega = 0.5$ (if the disc is cold), the reemitted flux may be as large as $F_{\text{dex}} = 0.5 F_{\text{abs}}$. Therefore in the subsequent calculations we took into account this effect and considered a fully relativistic treatment of this contribution to the overall line profile. Note that the magnitude of this correction may be overestimated in the Newtonian approximation. This is because in the real situation spontaneous emission from ions is Doppler boosted in the direction almost perpendicular to the line-of-sight (for low inclinations of the accretion disc relative to the observer) and the photons are preferentially radiated towards the accretion disc because of the light bending. Note that the above estimate is an upper limit also because the reabsorption of the line has been neglected.

We separately included the contribution to the iron line from spontaneous emission following absorption by taking into account the photons from the disc and the corona which were initially radiated in some other direction than that to the observer and later re-emitted into the line-of-sight. This was done by forward integrating the isotropic distribution of a large number of continuum and line photons from the whole corona located just above the disc and the whole disc respectively. For each trajectory and initial rest energy we localized the absorption regions and accumulated the absorbed luminosity in a large number of zones within the cloud. We assumed that either photons left the cloud without scattering or were scattered only once, i.e. we neglected the reabsorption of the line photons. This is a good approximation if the plasma is optically thin in the line. Note also that spontaneous emission which follows absorp-

tion produces photons at the energy of resonant transition and such photons are less likely to be further resonantly absorbed because of large energy shifts as seen by the local observers in the plasma. In other words, observers at some region in the absorbing plasma may see the re-emitted photons from other parts of the cloud at energies different from this of resonant transition and therefore such photons will not be reabsorbed. The total intercepted luminosity in any given zone within the cloud was calculated from (see also Ruszkowski 1999):

$$L(r, \theta) = \int \frac{\varepsilon(R)dS}{N} \sum_{i=1}^N Q(R, r, \theta), \quad (9)$$

where the summation is over all photon trajectories and emission energies, N is the total number of trajectories and dS is the surface area of an element of the corona as measured by the corotating observer:

$$dS = \gamma^{-1} \left(\frac{A}{\Delta} \right)^{1/2} \left(1 + \frac{2aV^{(\phi)}}{r\Delta^{1/2}} \right)^{-1} d\phi dr, \quad (10)$$

where γ and $V^{(\phi)}$ are the Lorentz factor and the azimuthal component of the velocity of the relative motion of the corona and the locally non-rotating observer. The remaining symbols have their usual meaning in the Kerr metric. The factor $Q(R, r, \theta)$ in Eq. 9 is:

$$Q(R, r, \theta) = \begin{cases} g_m^2 P_m EW_{em} \cos \beta & \text{for the line} \\ g_m^2 P_m dE_{em} & \text{for the continuum} \end{cases} \quad (11)$$

where m is the number of an absorption region for a given trajectory and emission energy and

$$P_m = (1 - e^{-\tau_m}) \prod_{i=0}^{m-1} e^{-\tau_i}. \quad (12)$$

The emission from the zones in the ionized cloud was then treated separately and each zone served as a source of line radiation. We calculated the observed flux by following a bundle of photons from a particular position within the cloud and computing the distortions of the solid angle $\Delta\Omega_{em}$ subtended by the surface element ΔS_{obs} on the observer's image plane as measured in the frame of reference of the emitter moving with the plasma flow. We used a formula similar to (4), i.e. :

$$F_{dex}(E_{obs})dE_{obs} = g^2 \frac{L(r, \theta)}{4\pi} \left. \frac{\partial\Omega_{em}}{\partial S_{obs}} \right|_i, \quad (13)$$

where the derivative was calculated at a fixed inclination i of the disc relative to the observer.

In order to obtain the overall line profile we added the fluxes calculated from Eq. 7 and Eq. 13. We also computed the observed equivalent widths of the lines by integrating the obtained profiles divided by the observed continuum.

3 RESULTS AND DISCUSSION

The examples of the computed iron line profiles for the parameters similar to that obtained by Nandra et al. (1999) for NGC 3516 are shown in Fig. 2 and Fig. 3. (Note that the exact values of the observed line equivalent widths are not known because the iron line in NGC 3516 varies on short

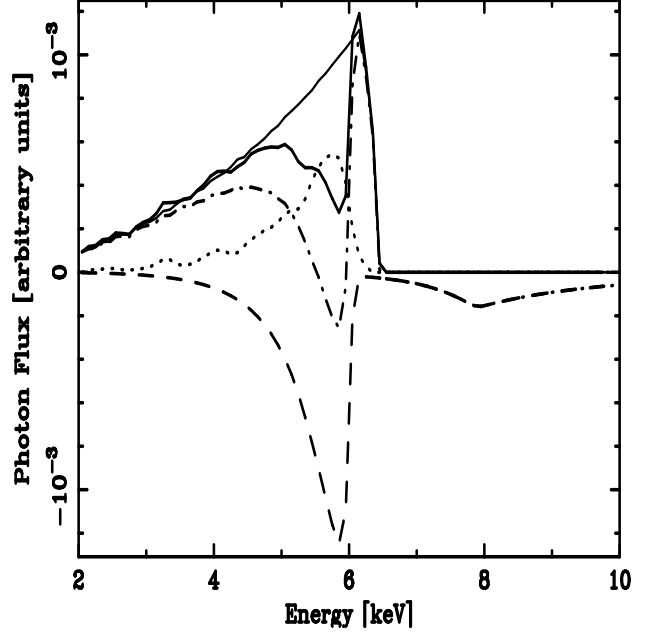


Figure 2. The iron line profile for: $i = 10^\circ$, $EW_{em} = 782$ eV, $\widetilde{EW}_{obs} = 510$ eV (unobscured; i.e. disc emission line only), $EW_{obs} = 398$ eV (obscured), $\Gamma = 3.0$, $\alpha = 0.5$, $r_{out} = 100m$ (outer radius of the disc, $R_c = 10m$, $N_H = 4 \times 10^{23} \text{ cm}^{-2}$, $a=0.998$, $A_{Fe} = 2A_{Fe\odot}$, absorption by He-like Fe ions; thin solid line - disc fluorescent line, thick solid line - resonantly absorbed disc fluorescent line, dashed line - resonant absorption of the continuum, dash-dotted line - disc fluorescent line absorbed by resonant and photoelectric absorption, dotted line - correction for spontaneous emission following absorption

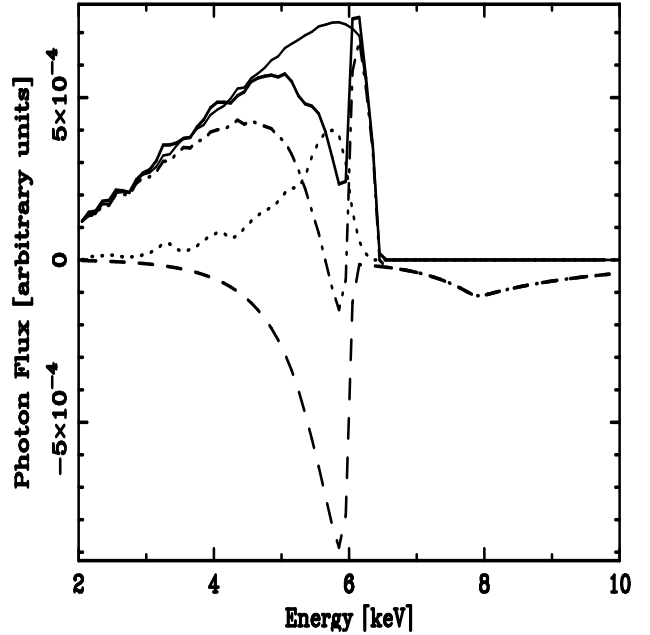


Figure 3. As Fig. 1 but for $EW_{em} = 1168$ eV, $\widetilde{EW}_{obs} = 698$ eV, $EW_{obs} = 578$ eV, $\Gamma = 3.25$

time scales and only time averaged equivalent width is reported in Nandra et al. 1999.) The thick red line denotes the total iron line profile (photon flux vs. energy). The shape of the line on Fig. 2 may provide an acceptable fit to the temporal profile obtained by Nandra et al. (1999) (compare with the inset in their Fig. 1). It peaks around 6.2 keV, has a long redshifted tail and possesses the redshifted absorption feature below 6.0 keV. As can be seen on Fig. 2, the observed redshift of the absorption feature can be mostly accounted for by the the strong gravitational redshift alone. This has to be contrasted with the main interpretation originally given by Nandra et al. (1999), who suggest that the redshift of the resonant absorption feature may be due to the scattering of radiation by matter infalling onto the black hole. Such matter would have to infall along the black hole rotation axis in order to efficiently absorb radiation from the central parts of the disc. Thus their interpretation implicitly implies accretion with low angular momentum which is less likely. Therefore our results suggest that the current observational data do not necessarily give the first direct evidence for the accretion of matter in AGNs.

The other profiles seen on the Fig. 2 and Fig. 3 correspond to different contributions to the total line profile, namely: disc fluorescent emission (thin solid line), resonant absorption of the continuum (dashed line) and correction for spontaneous emission from ions which follows absorption (dotted line). The dash-dotted line shows the disc line absorbed by resonant and photoelectric absorption (a small iron absorption edge created in the cloud is visible around 8 keV). Note that there is no intrinsic resonant absorption of the fluorescent disc emission line and only the continuum radiation is resonantly absorbed. This is the result of the low inclination of the disc. Emission line photons with rest energies at 6.4 keV leave the disc and continually move towards increasing gravitational potential and therefore their locally observed energies gradually decrease and can never exceed the rest energy of the resonant absorption line at 6.7 keV. Note also that the observed equivalent width of the emission line $\widetilde{EW}_{\text{obs}}$ (for the unabsorbed line) is smaller than the equivalent width EW_{em} measured face on in the local rest frame because of the gravitational redshift and the light bending which leads to the central parts of the disc being effectively observed at large angle even though the disc is seen at low inclination. The characteristic skewed shape of the profile of resonant absorption of the continuum is the result of the systematic effect of the gravitational redshift which creates the long redshifted tail and also due to variations of the Sobolev length across the disc as seen by the observer. The coherence length is larger for the photons on the approaching side of the disc and smaller on the opposite side because the cloud on the receding side has a velocity component directed away from the observer so the photons and plasma travel locally in opposite directions. Fig. 2 and Fig. 3 also show the contribution to the line from spontaneous emission following absorption. As expected, the profile of this line has a shape similar to that of the fluorescent disc line.

The line photons emitted by the cloud which impinge on the cold disc are thermalized and do not contribute to the final iron line profile. It has to be stressed that, in modelling NGC 3516, we assumed that the accretion disc was cold. The large observed equivalent widths of the order of 500 eV may

suggest an ionized disc, however a cold disc with an overabundance of iron and underabundance of other elements may still produce large equivalent widths of iron line by fluorescence from the illuminated disc material (Reynolds et al. 1995, Lee et al. 1999). The enhanced abundance of iron in the central regions of AGN is also plausible if one considers that in quasars large metallicities of up to 9 times the solar value have been inferred (Hamann & Ferland 1999). If however the accretion disc is ionized, two processes work in the opposite directions: 1) preferential illumination of the disc and efficient reflection of the line photons from the cloud and 2) Comptonization in the disc which smears this line. These two processes cancel each other to some extent. The continuum produced in the corona can also be reflected and later absorbed in the cloud which will lead to increases in the strengths of the continuum level, absorption feature and disc line by the same factor (for fixed EW_{em}). Note that even when the disc is ionized, the albedo may still be significantly far from unity. Thus, for an ionized accretion disc, resonant absorption is not completely cancelled by the correction for spontaneous emission.

The depth of the absorption feature depends on our parameter N_{H} which is related to the column density. The amount of ionized plasma which reprocesses the continuum and the emission line from the disc is constrained by the nondetection of the absorption edge of iron in the profiles obtained by Nandra et al. (1999). In order to estimate the importance of the absorption edge we calculate the factor $1 - e^{-\tau_{\text{edge}}} \approx \tau_{\text{edge}}$ where τ_{edge} is the optical depth at the photoionization threshold energy:

$$1 - e^{-\tau_{\text{edge}}} = 0.12 \left(\frac{f_{\text{H}} N_{\text{H}}}{10^{23} \text{cm}^{-2}} \right) \left(\frac{\sigma_{\text{edge}}}{2 \times 10^{-20} \text{cm}^2} \right) \left(\frac{A_{\text{Fe}}}{2A_{\text{Fe}\odot}} \right), \quad (14)$$

where σ_{edge} is the cross section for photoionization (σ_{H} and σ_{He} are both close to $2 \times 10^{-20} \text{cm}^2$, Yakovlev et al. 1992 and references therein). In consequence, the contrast of the absorption edge relative to the continuum can be small. The definition of N_{H} does not include the fact that the column densities for geodesics intersecting the cloud further away from the centre are smaller, which will also reduce the iron edge. It also has to be stressed that the contrast of any absorption edge created close to the black hole would be further reduced by a factor of a few by the strong relativistic effects operating in this region. We therefore calculate the iron edge using a fully relativistic treatment to determine the allowed values of N_{H} . The results are shown on Fig. 2 and Fig. 3 (dash-dotted lines around 8 keV). The strength of the calculated absorption edge is well within the acceptable range given the quality of the current data. In the considered range of temperatures the electrons in the plasma are nonrelativistic or mildly relativistic and the Thomson optical depth is $\tau_{\text{Th}} \approx 6.6 \times 10^{-2} (N_{\text{H}}/10^{23} \text{cm}^{-2})$ where N_{H} is the hydrogen column density. This means that the Compton y parameter $y = 4\tau_{\text{Th}}(1 + \tau_{\text{Th}})\Theta(1 + \Theta) \ll 1$, where $\Theta = kT/mc^2 = 1.7 \times 10^{-2} (T/10^8 \text{K}) \ll 1$ and thus, for the adopted values of N_{H} , Comptonization by the Thomson thin plasma is unlikely to significantly alter the energies of the emission line photons radiated by the accretion disc and the continuum in the range 2 – 10 keV (see also Fabian et al. 1995). As discussed above, the plasma may be photoionized

by the continuum radiation, so in addition to the above processes, fluorescence following photoionization in the cloud should in principle be considered. Its influence will however be small. It can be roughly estimated by calculating the ratio of the equivalent width for the fluorescent photons EW_f to the equivalent width for the resonant absorption EW_r in the Newtonian limit. In our model the plasma is effectively optically thin and in this regime the ratio EW_f/EW_r can be calculated by using the results from Matt (1994) and Krolik & Kallman (1987) and cast in the following form:

$$\frac{EW_f}{EW_r} = 0.14 \left(\frac{\sigma_{\text{edge}}}{2.0 \times 10^{-20} \text{cm}^2} \right) \left(\frac{\langle Y \rangle}{0.5 f_1} \right) \left(\frac{4}{3 + \alpha} \right) \times \left(\frac{(E/E_{\text{edge}})^\alpha}{0.9} \right) \left(\frac{E}{6.7 \text{keV}} \right) \left(\frac{\Delta\Omega/4\pi}{0.5} \right) \left(\frac{f_{\text{lu}}}{0.5} \right)^{-1}, \quad (15)$$

where $\langle Y \rangle$ is the fluorescent yield averaged over the fractional abundance of the iron ions (depending on temperature and some uncertain atomic physics (un the case of He-like Fe), Y_{H} and Y_{He} lie in the range $\approx 0.5 - 0.7$, Krolik 1999). α is the spectral energy index, E is the energy of the absorption/fluorescent line, E_{edge} is the threshold energy for photoionization and $\Delta\Omega$ is the solid angle subtended by the ionized plasma as seen by the primary continuum source. If the accretion disc is cold then the fluorescent photons created in the hot cloud are thermalized when they impinge upon the disc surface and are effectively destroyed and therefore $\Delta\Omega/4\pi = 0.5$. Similarly in the case of the hot disc, fluorescent photons directed towards the disc are strongly Comptonized by multiple scatterings in the hot, optically thick medium and the line spreads out to some extent and thus the effective value of $\Delta\Omega/4\pi < 1$. For example, the above ratio of the equivalent widths for $\alpha = 1$ can be as small as 0.065 in the case of the cold accretion disc surrounded by a hot plasma in which He-like ions are the primary source of opacity. Moreover, this is an upper limit because the reabsorption of the fluorescent photons has been neglected.

Fig. 4 shows the effect of the size of the cloud on the line profile. Large cloud sizes lead to stronger absorption because the coherence length over which resonant absorption can occur increases with distance from the black hole. Of course the smaller the cloud the greater the redshift of the absorption feature, but the magnitude of absorption decreases as the size of the cloud gets smaller. In principle, an ensemble of very small clouds or filaments distributed at a range of distances from the central black hole could produce a number of narrow absorption features superimposed on the emission line, an effect similar to the 'Ly α forest' observed in the spectra of distant quasars. It is indeed plausible that the absorbing plasma may exist in the form of small clumps. If the clumpy plasma of smoothed out mean density n_{H} is in photoionization equilibrium, the ionization parameter necessary to produce a high ionization state has to be $\xi = L_X / (n_{\text{H}} R_c^2) \sim 10^4$, where f is the filling factor. Assuming the X-ray luminosity (in the energy range 2-50 keV), the size of the absorbing region and the column density to be $L_X \sim 10^{43} \text{erg s}^{-1}$ (Stripe et al. 1998), $R_c \sim 10^{14} \text{cm}$ and $N_{\text{H}} \sim 10^{24} \text{cm}^{-2}$ respectively, one can obtain a rough estimate of the filling factor $f \propto \xi N_{\text{H}} R_c / L_X \sim 0.1$, implying that the plasma has a clumpy structure. We note that the free-free emission from

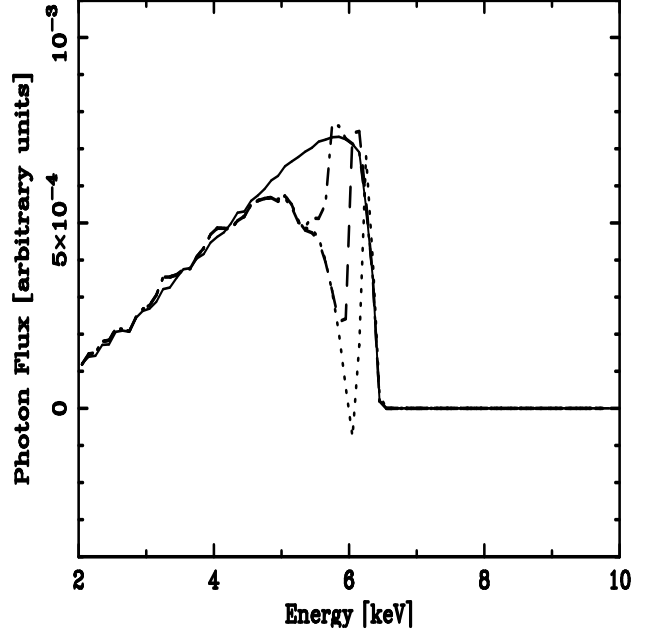


Figure 4. The iron line profiles for the same parameters and the same cloud density as in Fig. 2 (except for the equivalent widths) but for three different cloud sizes $R_c = 7\text{m}$ (dash-dotted line), 10m (dashed line), 13m (dotted line); thin solid line denotes disc fluorescent emission line profile

such clumps will be $L_{\text{ff}} \propto 10^{40} T_7^{1/2} \text{erg s}^{-1}$, much less than the luminosity in the X-ray band. Magnetic fields are a plausible mechanism of confinement of the clouds and we note that the existence of magnetically confined clumps above the accretion disc was proposed and extensively discussed by Kuncic, Celloti & Rees (1997). The cloud densities envisaged in our work are however much less extreme.

Recently Iwasawa et al. (1999) reported on the observations of the broad iron emission line in MCG-6-15-30. They observed a bright flare in the light curve during which the line peaked at 5 keV and most of the line emission was shifted below 6 keV with no component detected at 6.4 keV. They interpreted it as the result of an extraordinarily large gravitational redshift owing to a dominant flare occurring very close to the black hole at $r \approx 2\text{m}$. We speculate that their profile may also be explained by resonant absorption by the plasma expelled during the bright flare. It is conceivable that such highly ionized material may be ejected to larger heights above the accretion disc where the resonant absorption will be more efficient due to the larger coherence length. The weaker gravitational field at such distances will then lead to the absorption feature being less redshifted which may in turn cancel the main peak of the disc fluorescent emission line. Therefore the maximum of the profile of the partially absorbed iron line will be effectively seen at lower energies.

4 CONCLUSIONS

We have demonstrated that resonant absorption potentially plays an important role in the interpretation of the fluorescent iron emission line profiles from accreting black holes.

Our model can explain the absorption features seen in the profiles recently obtained by Nandra et al. (1999) giving an alternative explanation of the data whereby the redshift of the absorption features is mainly gravitational in origin and fast accretion of the matter along the spin axis of the black hole is not required. We hope that forthcoming data from Chandra X-ray Observatory may help to break the degeneracy of the two proposed scenarios. Future high signal-to-noise observations may also provide us with information about the accretion flow near the black hole.

5 ACKNOWLEDGMENTS

MR acknowledges support from an External Research Studentship of Trinity College, Cambridge; an ORS award; and the Stefan Batory Foundation. ACF thanks Royal Society for support. We thank Giorgio Matt, Roger Blandford and Martin Rees for useful discussions. We also thank the referee - H. Netzer for constructive comments.

REFERENCES

- Band D.L, Klein R.I., Castor J.I., Nash J.K., 1990, ApJ, 90
 Castor J.I., 1970, MNRAS, 149, 111
 Dabrowski Y., Fabian A.C., Iwasawa K., Lasenby A.N., Reynolds C.S., 1997, MNRAS, 288, L11
 Fabian A.C., Kunieda H., Inoue S., Matsuoka M., Mihara T., Miyamoto S., Otani C., Ricker G., Yamauchi M., Yaqoob T., 1994, PASJ, 46, L59
 Fabian A.C., Nandra K., Reynolds C.S., Brandt W.N., Otani C., Tanaka Y., Inoue H., Iwasawa K., 1995, MNRAS, 277, L11
 Hamann F., Ferland G.J., 1999, to appear in ARA&A and available at astro-ph/9904223
 Iwasawa K., Fabian A.C., Reynolds C.S., Nandra K., Otani C., Inoue H., Hayashida K., Brandt W.N., Dotani T., Kunieda H., Matsuoka M., Tanaka Y., 1996, MNRAS, 282, 1038
 Iwasawa K., Fabian A.C., Young A.J., Inoue H., Matsumoto C., 1999, MNRAS, 306, 19
 Kato T., 1976, ApJS, 30, 397
 Kuncic Z., Celotti A., Rees M.J., 1997, MNRAS, 717, 730
 Kurpiewski A., Jaroszyński M., 1999, A&A, 364, 713
 Krolik J.H., 1999, Active Galactic Nuclei: from the Central Black Hole to the Galactic Environment (Princeton: Princeton University Press)
 Krolik J.H., Kallman T.R., 1987, ApJL, 320, 5
 Lee J.C., Brandt W.N., Fabian A.C., Iwasawa K., Reynolds C.S., in preparation
 Lee J.C., Fabian A.C., Brandt W.N., Reynolds C.S., Iwasawa K., 1999, MNRAS, in press
 Matt G., 1994, MNRAS, 267, L17
 Morrison R., McCammon D., 1983, ApJ, 270, 119
 Mushotzky R.F., Fabian A.C., Iwasawa K., Kunieda H., Matsuoka M., Nandra K., Turner Y., 1995, MNRAS, 272, L9
 Nandra K., George I.M., Mushotzky R.F., Turner T.J., Yaqoob T., 1997, ApJ, 477, 602
 Nandra K., George I.M., Mushotzky R.F., Turner T.J., Yaqoob T., 1999, ApJL, in press, astro-ph/9907193
 Novikov I.D., Thorne K.S., 1993, in Black Holes [Les Houches Summer School 1972], DeWitt C. ed. (New York: Gordon and Breach Science Publishers)
 Reynolds C.S., 1997, MNRAS, 286, 513
 Reynolds C.S., Fabian A.C., Inoue H., 1995, MNRAS, 276, 1311
 Shu F.H., Physics of Astrophysics, Volume I: Radiation, 1991 (Mill Valley: University Science Books)
 Stripe G.M., Wilkes B.J., Comastri A., Mathur S., O'Brien P.T., 1998, in Scarsi H., Giommi P., Fiore F., ed., The Active X-Ray Sky: Results from BeppoSAX and RXTE, Nuclear Physics B Proceedings Supplements, 69, 505
 Tanaka Y. et al., 1995, Nature, 375, 659
 Yakovlev D.G., Band I.M., Trzhaskovskaya M.B., Verner D.A., ESO scientific preprint No. 835